HHS Public Access

Author manuscript

Neuroscience. Author manuscript; available in PMC 2023 August 21.

Published in final edited form as:

Neuroscience. 2022 August 21; 498: 93–104. doi:10.1016/j.neuroscience.2022.07.002.

Oxytocin receptors in the mouse centrally-projecting Edinger-Westphal nucleus and their potential functional significance for thermoregulation

Ju Li,

Andrey E Ryabinin

Department of Behavioral Neuroscience, Oregon Health & Science University, 3181 SW Sam Jackson Park Road, Portland, OR 97239, USA

Abstract

The centrally-projecting Edinger-Westphal nucleus (EWcp) has been shown to contribute to regulation of multiple functions, including responses to stress and fear, attention, food consumption, addiction, body temperature and maternal behaviors. However, receptors involved in regulation of these behaviors through EWcp remain poorly characterized. On the other hand, the oxytocin peptide (OXT) is also known to regulate a substantial number of physiological responses and behaviors. Here we show that mRNA encoding OXT receptors (Oxtr) is expressed in EWcp of male and female C57BL/6J mice. These receptors are present on urocortin 1 (Ucn) mRNA-containing neurons and, to a lesser extent, on neurons in EWcp expressing the vesicular glutamate transporter 2 (Vglut2) mRNA of EWcp. Using RNAscope in situ hybridization, we show that neurons containing Ucn and Vglut2 mRNAs are two intermingled, but independent subpopulations in EWcp and characterize their relationship with other populations of neurons in the vicinity of this nucleus. Using immunohistochemistry, we show that intraperitoneal (IP) administration of OXT can induce FOS in Oxtr-containing neurons, suggesting that these receptors on EWcp neurons are functional. A follow up study showed that injection of OXT (2.3 or 7.7 mg/kg, IP) is accompanied by a decrease in body temperature. Since EWcp is known to be involved in regulation of body temperature, we hypothesize that OXT's effects on body temperature could be mediated through the EWcp. The contribution of OXTR in EWcp to regulation of various functions of EWcp and OXT needs to be deciphered.

Keywords

Oxytocin; Edinger-Westphal nucleus; urocortin; glutamate; hypothermia; c-Fos

Corresponding Author: Andrey E Ryabinin, Ph.D., Department of Behavioral Neuroscience, Oregon Health & Science University, 3181 SW Sam Jackson Park Road, Portland, OR 97239, USA, ryabinin@ohsu.edu.

Introduction

Our understanding of relationships between various brain regions and their functions in behavior is continuing to expand. Relevant to this expansion is a developing appreciation that specific neuronal subpopulations within defined brain regions can have varied neurochemical nature and serve different roles. Such development is striking for the Edinger-Westphal nucleus (EW). Originally, EW was considered to be a parasympathetic cholingergic nucleus with very specific functions: constriction of pupil in response to light and lens accomodation, responses achieved through the innervation of ciliary ganglia (Edinger, 1855; Warwick, 1954; Westphal, 1887). While this narrow view was questioned early on, including by such visionaries as Ramon y Cajal (Cajal, 1995), this concept of the EW prevailed through the 20th century and is part of most neurology textbooks. This concept was finally challenged and revised when it was shown that EW contains other cells with projections to multiple brain regions (Bachtell et al., 2004; Loewy and Saper, 1978; Loewy et al., 1978) and does not contain markers for acetylcholine production in rodents, cats and humans (Cavani et al., 2003; Horn et al., 2008; May et al., 2008; Ryabinin and Weitemier, 2006; Weitemier and Ryabinin, 2005). As a result, the EW is now understood to refer to two populations of neurons: 1) the centrally-projecting EW (EWcp), which is not cholinergic, but is morphologically identical to the EW in human and rodent brain atlases, 2) the preganglionic EW (EWpg), which is cholinergic and anatomically well-defined in birds and monkeys (Kozicz et al., 2011).

While the EWpg serves its classical oculomotor function, the understanding of the functions of EWcp is less than clear. Early studies on EWcp, described its sensitivity to stress, alcohol and several other addictive drugs, and deduced its involvement in regulation of anxiety, depression, energy expenditure, thermoregulation and consummatory behaviors (Bachtell et al., 2002b; Bachtell et al., 1999; Bloem et al., 2012; Gaszner et al., 2004; Kozicz, 2003; Kozicz and Arimura, 2001; Weitemier and Ryabinin, 2005). More recent studies also indicate a role in attention, vigilance, fear responses and maternal behaviors (Li et al., 2018; Lovett-Barron et al., 2017; Priest et al., 2021; Topilko et al., 2022; Zhang et al., 2019). These expanding views on the functions of EWcp suggest that it is an important hub structure needing further exploration.

As the name suggests, EWcp was found to project not to the ciliary ganglia, but instead to a large number of central regions. Early studies described major projections from EWcp to include the spinal cord, the central nucleus of amygdala, the bed nucleus of stria terminalis, lateral septum, dorsal raphe and others (Bachtell et al., 2003; Bittencourt et al., 1999; da Silva et al., 2013; Dos Santos Junior et al., 2015; Kozicz, 2003; Maciewicz et al., 1984; Phipps et al., 1983; Weitemier et al., 2005). More recent studies suggest that the EWcp supplies major projections to the periaqueductal gray, caudate, lateral hypothalamus, supraoptic nucleus and other nuclei (Priest et al., 2021; Topilko et al., 2022).

The expanding views on the function and afferents of EWcp are paralleled by the increased appreciation for its neurochemical complexity. Thus, the most commonly known marker of EWcp neurons is urocortin 1 (UCN), a peptide of the corticotropin releasing family (Bittencourt et al., 1999; Vaughan et al., 1995). EWcp is the main source of UCN in

the brain (Kozicz et al., 1998; Weitemier et al., 2005; Wong et al., 1996). While no major neurotransmitters were identified as being expressed in UCN neurons, these neurons have also been shown to be one of the major brain sources of neuropeptide cocaine- and amphetamine-regulated transcript (CART) (Kozicz, 2003; Okere et al., 2010). Separate populations of neurons in the vicinity of EWcp were shown to contain tyrosine hydroxylase (TH) and vesicular glutamate transporter 2 (VGLUT2, also known as SLC17A6), a marker of glutamatergic neurons (Bachtell et al., 2002a; Fonareva et al., 2009; Spangler et al., 2009; Zhang et al., 2019). Some neurons in or near UCN were also found to contain the peptide cholecystokinin (CCK) (Innis and Aghajanian, 1986; Maciewicz et al., 1984). There appears to still be disagreement on whether CCK, UCN and VGLUT2 are markers for separate populations of neurons or could be co-expressed (Priest et al., 2021; Topilko et al., 2022; Zhang et al., 2019; Zuniga and Ryabinin, 2020).

The importance of EWcp for regulation of several functions requires attention to receptors that are expressed in this brain region. In agreement with its importance in regulation of energy expenditure and possible stress-related functions, earlier studies pointed to presence of ghrelin and leptin receptors in this brain region (Giardino et al., 2012; Scott et al., 2009; Spencer et al., 2012; Xu et al., 2009; Xu et al., 2022; Xu et al., 2011). Neurons of EWcp have also been shown to express estrogen beta receptors, suggesting potential sex-specific regulation of various functions (Derks et al., 2010). However, the receptor composition of neuronal populations of EWcp needs further exploration.

Here we describe the presence of receptors for oxytocin (OXT) in EWcp. OXT is nanopeptide well known to be involved in maternal behaviors, and more recently implicated in regulation of social behaviors, stress responses, nociception, food consumption, addictive behaviors and thermoregulation (Carter et al., 2020; Grinevich and Neumann, 2021; Lee et al., 2009). However, its receptors in EWcp have not been previously described. To bridge this gap in knowledge, we use RNAscope in situ hybridization (ISH) to investigate which neuronal populations in EWcp and its vicinity express OXT receptors (OXTRs). Since the relationship between various subpopulations of EWcp is a matter of disagreement, we also use RNAscope ISH to clarify the neuroanatomical relationships between several markers expressed in this area. To assess whether the OXTR receptors are functional, we tested whether peripheral administration of OXT results in FOS induction in EWcp neurons. Having identified EWcp as sensitive to administration of exogenous OXT, we tested whether administration of OXT is associated with hypothermic responses and FOS induction in EWcp.

Experimental Procedures

Animals.

Adult male and female C57BL/6J mice were obtained from Jackson Laboratories (Sacramento, CA, USA). They were housed in the main colony room at 4 per cage at 12/12 light:dark cycle (lights on at 6:00 am) in standard “shoebox” cages (18.4 cm W × 29.2 cm D × 12.7 cm H) in a temperature (20–22°C)- and humidity-controlled environment with food (LabDiet 5001; LabDiet) and water *ad libitum* prior to experiments for 1–2 weeks prior to experiments. All protocols were approved by the Oregon Health & Science University

animal care and use committee and performed within the National Institutes for Health Guidelines for the Care and Use of Laboratory Animals, as well as the Guidelines for the Care and Use of Mammals in Neuroscience and Behavioral Research.

RNAscope experiments.

To qualitatively characterize the presence of Oxtr mRNA in EWcp and to determine distribution of various markers in EWcp and its vicinity, we used 6 male and 6 female 10 weeks-old mice. Care was taken to ensure that analysis for each gene would be performed in both male and female mice. Mice were perfused by 4% paraformaldehyde in 10 mM phosphate-buffered saline (pH=7.4, PBS) and postfixed in the same solution for 24 hours at 4°C. The tissue was then immersed in 20% sucrose, and subsequently 30% sucrose/PBS at 4°C until tissue saturation was achieved. The brains were then frozen in Optimal Cutting Temperature (OCT) embedding media in 2-methylbutane with dry ice, and stored in an airtight container at −80°C. Slices were cut with a CM1950 cryostat (Leica Microsystems, Inc., Deerfield, IL) at 12–15 μm thickness.

The RNA scope ISH is based on patented signal amplification and background suppression technology by Advanced Cell Diagnostics, Inc (ACD). We followed the manual for the RNAscope® Multiplex Fluorescent Reagent Kit v2 (Cat. No. 323100) for fixed frozen tissue mounted on slides. The validated probes for specific mouse mRNAs were designed by ACD and are listed in Table 1. The gene probes were combined with different fluorescent dies (Akoya Biosciences - FP1487001KT - Opal 520, Akoya Biosciences - FP1488001KT - Opal 570) to enable double-labeling when needed. Autofluorescence and non-specific binding was eliminated by a 15 mins at 40°C incubation with RNAscope® Multiplex FL v2 HRP blocker (included in kit).

Slides were washed in PBS and baked for 30 minutes at 60°C. Sections were post-fixed by immersing the slides in prechilled 10% neutral-buffered formalin for at 4°C. Slides were then dehydrated through serial incubations in 50% ethanol (EtOH), 70% EtOH, 100% EtOH, then again 100% EtOH and air-dried for 5 min at room temperature. To improve the gene signal, fresh RNAscope® 1X Target Retrieval Reagent (included in kit 323100) was applied for a 5-minute incubation at 98–102°C. The hot slides were then transferred into distilled water and rinsed two times, followed by one rinse in 100% EtOH, before being air dried. A barrier around brain sections was drawn using ImmEdge Hydrophobic Barrier pen. RNAscope Protease III was applied to section for 30 min at 40°C to expose mRNA. Following this, slides were rinsed two times with distilled water. Incubation with each probe was done for 2 hours at 40°C. At the same time, sections were incubated with the 3-plex positive control probe (Cat No: 320881) and the 3-plex Negative Control Probe (Cat No: 320871) with each assay. The slides were washed two times in the provided Wash buffer (ACD, 310091) for 2 minutes each.

Amplification and detection steps were performed using the RNAscope Multiplex Fluorescent Reagent Kit v2 for single-plex probes. Sections on slides were incubated with Amp1 and then Amp2 for 30 min at 40°C and then washed two times in Wash buffer for 2 minutes each between both incubations. Amp3 was applied onto the sections for a 15-minute incubation at 40°C, followed by two washes in Wash buffer for 2 min each. The reaction

was developed with channel-appropriate solutions for 15 minutes at 40°C and then washed two times for 2 minutes each. For product detection, 50–100μL of diluted Opal 520/570 (1: 2200) was added to each slide and incubated for 30 minutes at 40°C. The slides were again washed with Wash solution two times. For double labeling, steps starting with Amp1 to Opal 520/570 were repeated. The slides were washed two times as described above, followed by the blocking procedure as mentioned above and washed two times as well. After the final two washes, each slice was immediately covered with 1–2 drops of ProLong Gold Antifade Mountant.

FOS immunohistochemistry after OXT injection—To test whether OXT administration results in FOS induction in EWcp, we performed an immunohistochemistry (IHC) experiment. The study was performed with 4 male and 4 females per treatment (8 weeks of age) during the light phase of the circadian cycle. Mice were habituated to daily intraperitoneal (IP) saline injections for 2 days prior to experiment. On the day of experiment, mice were injected either 7.7 mg/kg OXT (IP) or corresponding volume of saline. Ninety minutes after the injection, mice were euthanized by CO_2, brains dissected and post-fixed in 2% PFA/1xPBS. Immersion rather than perfusion was used because it allows quicker dissection times and processing more brains at a time, which decreases batch effects. The rest of the IHC procedure was as described previously (Robins et al., 2020). Brain slices were sectioned at 30 μm across the entire midbrain section corresponding to approximate Bregma levels from − 2.7 mm to − 4 mm. Nine representative sections were analyzed for each animal: 3 for anterior EWcp (~Bregma level −2.9 mm), 3 for middle EWcp (~Bregma level −3.3 mm) and 3 for posterior EWcp (~Bregma level −3.7 mm). Rabbit polyclonal anti-FOS antibody (F7799, Millipore-Sigma, St Louis, MO, 1:12000 in PBS/Triton-100/Bovine Serum Albumin) was used as the primary antibody. Immunological reactions were visualized with the 3,3'-diaminobenzidine tetrahydrochloride substrate solution (Pierce DAB Substrate kit, ThermoFisher Scientific, Waltham, MA). Control reactions performed without the anti-FOS antibody did not result in presence of positive staining. FOS-positive cells were identified by intense dark nuclear staining. The number of FOS-positive cells were counted for each Bregma level (anterior, middle and posterior). The numbers for each level across of EWcp were averaged for each animal to obtain a single data point per Bregma level, which was used for statistical analysis. Two-way repeated ANOVA (between-subjects factors: treatment and sex, repeated within-subject factor: Bregma level) was used to assess the effects statistically. Fisher PLSD was used as a post-hoc test. For this and subsequent quantitative analyses effects sizes are indicated by $\eta 2$. In parallel to the FOS IHC experiment, a separate set of 2 male and 2 female mice underwent an identical experiment, but brains were collected for RNAscope ISH (as described in the section above) to qualitatively assess for colocalization of *c-Fos* mRNA with either *Ucn* mRNA or *Oxtr* mRNA.

Hypothermia experiment—To test whether activation of EWcp by OXT, manifested in FOS induction, was associated with changes in body temperature, a separate set of male and female mice (3 per sex per treatment) were tested for hypothermic effects of OXT after injection of 2.3 mg/kg, or 7.7 mg/kg of OXT, or 3 g/kg EtOH (positive control) or saline (8 weeks old, 3 mice per sex per treatment). Animals were habituated to saline

injections and two rectal body temperature measurements during the two days prior to the experiment. On the day of experiment, animals received corresponding injections and rectal body temperatures were assessed at 30 min and 90 minutes after injections. 2-way repeated ANOVA (between-subject factors: treatment and sex, within-subject factor: time) was used to analyze body temperature. Significant effects were followed by Fisher's PLSD post-hoc tests. Animals were euthanized after the second body temperature measurement and IHC was performed to test whether the observed effects on body temperature were accompanied by changes in the number of FOS-positive neurons in EWcp. In these experiments, slides were coded such that the person performing the counts was unaware of groups assignment of analyzed images. FOS IHC was performed and analyzed as described above.

Results

Characterization of midbrain Oxtr expression and neuronal populations of EWcp.

Qualitative analysis of *Oxtr* mRNA localization by RNAscope ISH in the mouse midbrain revealed several prominent locations of its expression, such as the ventral hippocampus, amygdalohippocampal areas, several cortical areas, and the periaqueductal gray, especially its ventral portion, including the EWcp (Fig 1A–C). Since the cortical, amygdalar and hippocampal areas of *Oxtr* mRNA expression have been described in previous studies, we focused on the ventral central gray. Because EWcp is the major site of expression of UCN, we confirmed by RNAscope ISH that all *Ucn*-positive neurons of EWcp contained *Oxtr* (Fig 1D–F). The *Oxtr* mRNA was also expressed at what appeared a slightly lower levels in neurons surrounding the UCN EWcp neurons (Fig 1F, I).

The neurotransmitter nature of neuronal populations in the EWcp and its vicinity is still incompletely characterized and is a matter of controversy. Therefore, we performed RNAscope ISH to characterize independent populations of neurons in this area. Expression of paired markers was analyzed as separate images and as merged images to evaluate co-labelling. (Fig 2). We performed the characterization on a qualitative level in both male and female C57BL/6J mice across three major Bregma levels corresponding to anterior EWcp (sometimes also designated as pre-EW in atlases, Bregma level −2.9 mm), middle EWcp (also designated in atlases as pre-EW, Bregma level −3.3) and posterior EWcp (designated in atlases as EW, Bregma level −3.7) (Fig 3). No double labeled cells containing *Ucn* mRNA and *Vglut2* mRNA were detected. Therefore, the population of UCN neurons of EWcp was independent of the population of VGLUT2 neurons. We noted, however, that *Vglut2* mRNA-positive cells were at times intermingled with UCN neurons (Fig 2A–C, Fig 3A–C). The *Oxtr* mRNA was also double-labeled with some of the *Vglut2* mRNA-positive neurons (Fig 1H–J). The neurons expressing the mRNAs for peptides CART and CCK both completely overlapped with the UCN population (Fig 2D–F, Fig 3D–E). The *Cck* mRNA-containing neurons did not overlap with the *Vglut2* mRNA-positive population (Fig. 3F). Thus, the UCN/CART/CCK cells are independent from the local VGLUT2 neurons. The GABAergic neurons expressing *Gad1* mRNA were located dorsolateral to *Ucn* mRNA-containing neurons and were considered outside of EWcp (Fig 2G–I, Fig 3G). A few GABAergic neurons expressing *Gad2* mRNA were detected within the EWcp, but they did not co-express *Ucn* mRNA. Lower intensity *Gad2* mRNA-positive signal was also detected

dorsolateral to UCN neurons (Fig 3H). The tyrosine hydroxylase (*Th*) mRNA-positive neurons were rare and a few intermingled with *Ucn* mRNA-containing neurons (Fig 3I). The Choline acetyl transferase (*Chat*) mRNA -positive neurons in the oculomotor nucleus were completely independent from the UCN/CART/CCK neurons and were located lateral to the EWcp neurons (Fig 2J–L, Fig 3J–L).

The Oxtr mRNA-containing neurons respond to high doses of exogenous OXT

—To evaluate whether the OXTR in EWcp is functionally significant, we tested whether neurons of EWcp would be activated following an exogenous administration of this peptide. To test this possibility, we investigated FOS immunoreactivity in the midbrain of male and female mice (4 mice per treatment) following an IP injection of 7.7 mg/kg OXT (Fig 4). Qualitative observations indicated that there was no noticeable FOS signal in areas that did not express *Oxtr* mRNA, such as substantia nigra (SNR, Fig 1A and Fig 4F). There was also very sparse induction of FOS in the hippocampal areas (Fig 4E), despite very high levels of *Oxtr* mRNA in them (Fig 1A). The EWcp (Fig 4A–C), as well as the periaqueductal gray (Fig 4D) were robustly responsive to OXT administration. A 2-way ANOVA performed on the number of FOS-positive cells in EWcp (Fig 5A,B) confirmed a significant effect of treatment on this number ($F_{1,12}$=18.09, p=0.001, η^2=0.60), with no effect of sex or sex by treatment interaction. There was also a significant effect of Bregma level on the number of FOS cells ($F_{2,24}$=28.27, p<0.001, η^2=0.72) as well as a significant Bregma level by treatment interaction on this measure ($F_{2,24}$=4.64, p=0.02, η^2=0.28), but no other interactions with the repeated factor. Fisher's PLSD post-hoc analysis revealed that the effects and interactions of Bregma level were due to higher FOS numbers in posterior regions versus anterior regions and, as a consequence, significant differences between the saline and OXT groups in mid-EWcp and posterior EWcp (Fig 5A,B).

Qualitative RNAscope ISH analysis on an additional set of mice (2 mice per sex) confirmed that OXT induced *c-Fos* mRNA in *Oxtr* mRNA-containing and *Ucn* mRNA-containing neurons (Fig 4G–L).

Sensitivity of EWcp neurons to exogenous OXT is associated with hypothermic responses and FOS induction.

To test whether FOS induction in EWcp after OXT injections is associated with differences in OXT's hypothermic effects, we assessed changes in body temperature after injections of 2.3 or 7.7 mg/kg of OXT at 30 and 90 minutes after injection. As a positive control, we also studied effects of 3 g/kg of EtOH (3 g/kg, IP) at the same time points (Fig 5C,D). As expected, EtOH administration produced a robust hypothermic effect across both analyzed times. The higher dose of OXT produced a robust, but short-term hypothermic effect resulting in lower body temperature at 30 minutes, but not at 90 minutes post-injection. The lower dose of OXT, resulted in lower, but more varied, body temperature at 30 minutes and did not produce hypothermia at 90 minutes post-injection. Two-way repeated ANOVA showed no overall significant effects of treatment or sex, or interactions between them. However, there was a significant effect of time ($F_{1,16}$=24.40, p<0.001, η^2=0.60) and a significant time by treatment interaction ($F_{3,16}$=7.40, p=0.003, η^2=0.58). Fisher's PLSD post-hoc tests indicated highly significant decreases in body temperature at both

30 minutes (p=0.0022) and 90 minutes (p=0.011) after EtOH injection versus saline for both sexes. The 7.7 mg/kg OXT resulted in significantly lower temperature levels versus saline at 30 minutes in male (p=0.008) and female animals (p=0.003). The 2.3 mg/kg OXT resulted in statistically significantly lower body temperature in female animals versus saline at 30 minutes post-injection (p=0.015), but not in any other comparisons (Fig 5C). Following assessment of changes in body temperature, we also analyzed levels of FOS immunoreactivity in these animals. Both 2.3 and 7.7 mg/kg doses of the OXT resulted in significant FOS induction (Table 2). Injection of EtOH resulted in an even more robust FOS induction compared to OXT injections.

Discussion

These results demonstrate that UCN-containing neurons, and to a lesser extent VGLUT2 neurons of the EWcp, express OXTRs. Based on our observation that exogenous administration of high doses of OXT results in FOS induction in these neurons, we suggest that these OXTR are functionally significant. This induction is accompanied by a reduction in body temperature, which suggest that OXT actions on these receptors could result in hypothermia.

In addition, our studies have clarified the composition of neuronal populations within and in the vicinity of EWcp. UCN and CART have been previously shown to colocalize in the EWcp and form its main group of neurons (Kozicz, 2003). On the other hand, while early research suggested that peptides UCN and CART are co-expressed with CCK in the EWcp (Giardino et al., 2012), other studies concluded that CCK neurons express *Vglut2* mRNA (Zhang et al., 2019). This observation, in turn suggested that at least some of UCN neurons could express VGLUT2, and, therefore, could be glutamatergic. We find no evidence of *Cck* mRNA outside of *Ucn* mRNA-positive neurons of EWcp and no colocalization between the *Cck* and *Vglut2*. This finding is in agreement with more recent studies showing that UCN/CCK/CART neurons form a population of neurons distinct from *Vglut2*-positive cells, and, therefore, are unlikely to be glutamatergic (Giardino et al., 2012; Priest et al., 2021; Topilko et al., 2022). Other neurons in the vicinity of EWcp are thought to produce acetylcholine, dopamine or GABA. The lack of colocalization between UCN and CHAT immunoreactivity was one the crucial reasons leading to identification of EWcp as a separate entity from the cholinergic EWpg (Horn et al., 2008; May et al., 2008; Ryabinin et al., 2005; Weitemier and Ryabinin, 2005). The lack of colocalization between TH and UCN based on immunohistochemical evidence has also been discussed previously (Bachtell et al., 2002a; Spangler et al., 2009; Zuniga and Ryabinin, 2020). The lack of *Gad1* and *Gad2* colocalization with UCN also suggests that UCN neurons are not GABAergic, a finding in agreement with recent conclusive evidence showing that UCN neurons of EWcp are one of a few neuronal populations that express peptides, but do not produce any major neurotransmitters (Priest et al., 2021; Topilko et al., 2022).

We show here for the first time, that OXTRs are present on UCN neurons of EWcp and, perhaps to a lesser extent on the VGLUT2 neurons in the region. OXTRs are seven transmembrane receptors signaling through the Galpha cascade. It is expected, therefore, that activation of OXTRs should result in activation of cells that express them (Grinevich

and Ludwig, 2021). Indeed, we observe here that IP administration of a OXT (2.3 or 7.7 mg/kg) results in FOS induction in this area. This dose is higher than doses required to produce many behavioral effects (Carter et al., 2020; Grinevich and Neumann, 2021). However, OXT doses up to 10 mg/kg (IP) are anxiolytic in mice (Ring et al., 2006), which makes it unlikely that OXT produces c-Fos induction due to an unspecific stress-like response to this administration. The other argument against non-specific effects of OXT is the selectivity of FOS induction in specific brain regions. Thus, hippocampus is known to respond to stressful stimuli. However, OXT-induced FOS in this brain region is minimal. There is controversy about how well and through what mechanisms peripherally-administered OXT reaches specific brain regions (Bowen et al., 2011; Richard et al., 1991). However, studies in mice definitively show that IP administration of OXT results in penetration of the labelled peptide into the brain (Smith et al., 2019). While we can't completely exclude that activation of EWcp is an indirect consequence of OXT's actions outside of this brain region, the presence of OXTR in EWcp and their activation by exogenously-administered OXT suggest that these cells respond to endogenous OXT. The main sites of OXT production in mammalian brain are the paraventricular nucleus, supraoptic nucleus and, to a lesser extent, accessory nucleus of hypothalamus. However, our knowledge of the neurocircuitry of OXT is currently undergoing substantial revisions, such that OXT is thought to mediate its actions not only through synaptic, but also non-synaptic innervation and dendritic release (Grinevich and Ludwig, 2021).The source of OXT innervating EWcp needs to be determined.

Oxtr mRNA was robustly expressed in the *Ucn*-positive cells of EWcp, but was also present in nearby cells, some of which are *Vglut2*-positive. Both of these populations have been shown to contribute to thermoregulation. Thus, UCN immunoreactivity in EWcp correlates with hypothermic response to EtOH in "COLD" and "HOT" mice selectively-bred for this response and in the heterogeneous F2 generation of B6 × D2 genetic cross. These findings suggest that UCN levels in EWcp are associated with EWcp activation-induced hypothermia (Bachtell et al., 2002b). On the other hand, chemogenetic stimulation of *Vglut2*-producing cells of EWcp also results in hypothermia (Zuniga et al., 2021). Electrolytic lesions of EWcp, which do not distinguish between UCN and VGLUT2 neurons of EWcp, inhibit EtOH-induced hypothermia (Bachtell et al., 2004). In the opposite direction, pharmacological inhibition on EWcp by local administration of muscimol and baclofen, which also does not distinguish between UCN and VGLUT2 neurons of EWcp, increased body temperature (Zuniga et al., 2020). Microinfusion studies suggest that the UCN neurons of EWcp contribute to hypothermia via release of UCN in the dorsal raphe (Turek and Ryabinin, 2005), but it is also possible that UCN- and Vglut2-positive neurons act in tandem to decrease body temperature. Our experiments are correlative in nature and do not establish that OXT acting on OXTR in EWcp regulates body temperature in a causative manner. However, they suggest this possibility.

Taken together, our studies show that UCN and VGLUT2 neurons in and around EWcp are two independent, but intermingled, subpopulations of neurons. Both of these populations express OXTR. Our studies suggest that this OXTR in EWcp is functional, such that its binding results in activation of these cells and is accompanied by physiological effects. Temporary hypothermia resulting from exogenous OXT could be due to effects on OXTR

in EWcp. The functional contribution of OXTR in EWcp to the roles of OXT and EWcp in behavior and physiological responses needs to be further understood.

Acknowledgement

This study was supported by NIH Grants R01 AA019793, R01 AA025024 and R01 AA028680 (to AER).

References

Bachtell RK, Tsivkovskaia NO, and Ryabinin AE (2002a). Alcohol-induced c-Fos expression in the Edinger-Westphal nucleus: pharmacological and signal transduction mechanisms. J Pharmacol Exp Ther 302, 516–524. [PubMed: 12130710]

Bachtell RK, Tsivkovskaia NO, and Ryabinin AE (2002b). Strain differences in urocortin expression in the Edinger-Westphal nucleus and its relation to alcohol-induced hypothermia. Neuroscience 113, 421–434. [PubMed: 12127099]

Bachtell RK, Wang YM, Freeman P, Risinger FO, and Ryabinin AE (1999). Alcohol drinking produces brain region-selective changes in expression of inducible transcription factors. Brain Res 847, 157–165. [PubMed: 10575084]

Bachtell RK, Weitemier AZ, Galvan-Rosas A, Tsivkovskaia NO, Risinger FO, Phillips TJ, Grahame NJ, and Ryabinin AE (2003). The Edinger-Westphal-lateral septum urocortin pathway and its relationship to alcohol consumption. J Neurosci 23, 2477–2487. [PubMed: 12657708]

Bachtell RK, Weitemier AZ, and Ryabinin AE (2004). Lesions of the Edinger-Westphal nucleus in C57BL/6J mice disrupt ethanol-induced hypothermia and ethanol consumption. Eur J Neurosci 20, 1613–1623. [PubMed: 15355328]

Bittencourt JC, Vaughan J, Arias C, Rissman RA, Vale WW, and Sawchenko PE (1999). Urocortin expression in rat brain: evidence against a pervasive relationship of urocortin-containing projections with targets bearing type 2 CRF receptors. J Comp Neurol 415, 285–312. [PubMed: 10553117]

Bloem B, Xu L, Morava E, Faludi G, Palkovits M, Roubos EW, and Kozicz T (2012). Sex-specific differences in the dynamics of cocaine- and amphetamine-regulated transcript and nesfatin-1 expressions in the midbrain of depressed suicide victims vs. controls. Neuropharmacology 62, 297–303. [PubMed: 21803054]

Bowen MT, Carson DS, Spiro A, Arnold JC, and McGregor IS (2011). Adolescent oxytocin exposure causes persistent reductions in anxiety and alcohol consumption and enhances sociability in rats. PLoS One 6, e27237. [PubMed: 22110618]

Cajal S.R.y. (1995). Histology of the Nervous System of Man and Vertebrates, 1 edn (New York: Oxford University Press).

Carter CS, Kenkel WM, MacLean EL, Wilson SR, Perkeybile AM, Yee JR, Ferris CF, Nazarloo HP, Porges SW, Davis JM, et al. (2020). Is Oxytocin "Nature's Medicine"? Pharmacol Rev 72, 829–861. [PubMed: 32912963]

Cavani JA, Reiner A, Cuthbertson SL, Bittencourt JC, and Toledo CA (2003). Evidence that urocortin is absent from neurons of the Edinger-Westphal nucleus in pigeons. Braz J Med Biol Res 36, 1695–1700. [PubMed: 14666254]

da Silva AV, Torres KR, Haemmerle CA, Cespedes IC, and Bittencourt JC (2013). The Edinger-Westphal nucleus II: Hypothalamic afferents in the rat. J Chem Neuroanat 54, 5–19. [PubMed: 23619059]

Derks NM, Gaszner B, Roubos EW, and Kozicz LT (2010). Sex differences in urocortin 1 dynamics in the non-preganglionic Edinger-Westphal nucleus of the rat. Neurosci Res 66, 117–123. [PubMed: 19833156]

Dos Santos Junior ED, Da Silva AV, Da Silva KR, Haemmerle CA, Batagello DS, Da Silva JM, Lima LB, Da Silva RJ, Diniz GB, Sita LV, et al. (2015). The centrally projecting Edinger-Westphal nucleus--I: Efferents in the rat brain. J Chem Neuroanat 68, 22–38. [PubMed: 26206178]

Edinger L (1855). Uber den Verlauf der centralen Hirnnervenbahnen mit Demonstrationen von Preparaten. Arch Psychiatr Nervenkrankheiten 16, 858–859.

Fonareva I, Spangler E, Cannella N, Sabino V, Cottone P, Ciccocioppo R, Zorrilla EP, and Ryabinin AE (2009). Increased perioculomotor urocortin 1 immunoreactivity in genetically selected alcohol preferring rats. Alcohol Clin Exp Res 33, 1956–1965. [PubMed: 19673740]

Gaszner B, Csernus V, and Kozicz T (2004). Urocortinergic neurons respond in a differentiated manner to various acute stressors in the Edinger-Westphal nucleus in the rat. J Comp Neurol 480, 170–179. [PubMed: 15514930]

Giardino WJ, Cote DM, Li J, and Ryabinin AE (2012). Characterization of Genetic Differences within the Centrally Projecting Edinger-Westphal Nucleus of C57BL/6J and DBA/2J Mice by Expression Profiling. Front Neuroanat 6, 5. [PubMed: 22347848]

Grinevich V, and Ludwig M (2021). The multiple faces of the oxytocin and vasopressin systems in the brain. J Neuroendocrinol 33, e13004. [PubMed: 34218479]

Grinevich V, and Neumann ID (2021). Brain oxytocin: how puzzle stones from animal studies translate into psychiatry. Mol Psychiatry 26, 265–279. [PubMed: 32514104]

Horn AK, Eberhorn A, Hartig W, Ardeleanu P, Messoudi A, and Buttner-Ennever JA (2008). Perioculomotor cell groups in monkey and man defined by their histochemical and functional properties: reappraisal of the Edinger-Westphal nucleus. J Comp Neurol 507, 1317–1335. [PubMed: 18186030]

Innis RB, and Aghajanian GK (1986). Cholecystokinin-containing and nociceptive neurons in rat Edinger-Westphal nucleus. Brain Res 363, 230–238. [PubMed: 3942895]

Kozicz T (2003). Neurons colocalizing urocortin and cocaine and amphetamine-regulated transcript immunoreactivities are induced by acute lipopolysaccharide stress in the Edinger-Westphal nucleus in the rat. Neuroscience 116, 315–320. [PubMed: 12559087]

Kozicz T, and Arimura A (2001). Axon terminals containing CGRP-immunoreactivity form synapses with CRF- and Met-enkephalin-immunopositive neurons in the laterodorsal division of the bed nucleus of the stria terminalis in the rat. Brain Res 893, 11–20. [PubMed: 11222987]

Kozicz T, Bittencourt JC, May PJ, Reiner A, Gamlin PD, Palkovits M, Horn AK, Toledo CA, and Ryabinin AE (2011). The Edinger-Westphal nucleus: a historical, structural, and functional perspective on a dichotomous terminology. J Comp Neurol 519, 1413–1434. [PubMed: 21452224]

Kozicz T, Yanaihara H, and Arimura A (1998). Distribution of urocortin-like immunoreactivity in the central nervous system of the rat. J Comp Neurol 391, 1–10. [PubMed: 9527535]

Lee HJ, Macbeth AH, Pagani JH, and Young WS 3rd (2009). Oxytocin: the great facilitator of life. Prog Neurobiol 88, 127–151. [PubMed: 19482229]

Li X, Chen W, Pan K, Li H, Pang P, Guo Y, Shu S, Cai Y, Pei L, Liu D, et al. (2018). Serotonin receptor 2c-expressing cells in the ventral CA1 control attention via innervation of the Edinger-Westphal nucleus. Nat Neurosci 21, 1239–1250. [PubMed: 30104733]

Loewy AD, and Saper CB (1978). Edinger-Westphal nucleus: projections to the brain stem and spinal cord in the cat. Brain Res 150, 1–27. [PubMed: 78743]

Loewy AD, Saper CB, and Yamodis ND (1978). Re-evaluation of the efferent projections of the Edinger-Westphal nucleus in the cat. Brain Res 141, 153–159. [PubMed: 624070]

Lovett-Barron M, Andalman AS, Allen WE, Vesuna S, Kauvar I, Burns VM, and Deisseroth K (2017). Ancestral Circuits for the Coordinated Modulation of Brain State. Cell 171, 1411–1423 e1417. [PubMed: 29103613]

Maciewicz R, Phipps BS, Grenier J, and Poletti CE (1984). Edinger-Westphal nucleus: cholecystokinin immunocytochemistry and projections to spinal cord and trigeminal nucleus in the cat. Brain Res 299, 139–145. [PubMed: 6202372]

May PJ, Reiner AJ, and Ryabinin AE (2008). Comparison of the distributions of urocortin-containing and cholinergic neurons in the perioculomotor midbrain of the cat and macaque. J Comp Neurol 507, 1300–1316. [PubMed: 18186029]

Okere B, Xu L, Roubos EW, Sonetti D, and Kozicz T (2010). Restraint stress alters the secretory activity of neurons co-expressing urocortin-1, cocaine- and amphetamine-regulated transcript peptide and nesfatin-1 in the mouse Edinger-Westphal nucleus. Brain Res 1317, 92–99. [PubMed: 20043894]

Phipps BS, Maciewicz R, Sandrew BB, Poletti CE, and Foote WE (1983). Edinger-Westphal neurons that project to spinal cord contain substance P. Neurosci Lett 36, 125–131. [PubMed: 6191256]

Priest MF, Freda SN, Badong D, Dumrongprechachan V, and Kozorovitskiy Y (2021). Peptidergic modulation of fear responses by the Edinger-Westphal nucleus. bioRxiv 2021.2008.2005.455317.

Richard P, Moos F, and Freund-Mercier MJ (1991). Central effects of oxytocin. Physiol Rev 71, 331–370. [PubMed: 1672455]

Ring RH, Malberg JE, Potestio L, Ping J, Boikess S, Luo B, Schechter LE, Rizzo S, Rahman Z, and Rosenzweig-Lipson S (2006). Anxiolytic-like activity of oxytocin in male mice: behavioral and autonomic evidence, therapeutic implications. Psychopharmacology (Berl) 185, 218–225. [PubMed: 16418825]

Robins MT, Li J, and Ryabinin AE (2020). Effects of Housing Conditions and Circadian Time on Baseline c-Fos Immunoreactivity in C57BL/6J Mice. Neuroscience 431, 143–151. [PubMed: 32081725]

Ryabinin AE, Tsivkovskaia NO, and Ryabinin SA (2005). Urocortin 1-containing neurons in the human Edinger-Westphal nucleus. Neuroscience 134, 1317–1323. [PubMed: 16039794]

Ryabinin AE, and Weitemier AZ (2006). The urocortin 1 neurocircuit: ethanol-sensitivity and potential involvement in alcohol consumption. Brain Res Rev 52, 368–380. [PubMed: 16766036]

Scott MM, Lachey JL, Sternson SM, Lee CE, Elias CF, Friedman JM, and Elmquist JK (2009). Leptin targets in the mouse brain. J Comp Neurol 514, 518–532. [PubMed: 19350671]

Smith AS, Korgan AC, and Young WS (2019). Oxytocin delivered nasally or intraperitoneally reaches the brain and plasma of normal and oxytocin knockout mice. Pharmacol Res 146, 104324. [PubMed: 31238093]

Spangler E, Cote DM, Anacker AM, Mark GP, and Ryabinin AE (2009). Differential sensitivity of the perioculomotor urocortin-containing neurons to ethanol, psychostimulants and stress in mice and rats. Neuroscience 160, 115–125. [PubMed: 19248818]

Spencer SJ, Xu L, Clarke MA, Lemus M, Reichenbach A, Geenen B, Kozicz T, and Andrews ZB (2012). Ghrelin regulates the hypothalamic-pituitary-adrenal axis and restricts anxiety after acute stress. Biol Psychiatry 72, 457–465. [PubMed: 22521145]

Topilko TD, Diaz SL, Pacheco CM, Verny F, Kirst C, Rousseau C, Deleuze C, Gaspar P, and Renier N (2022). Edinger-Westphal Peptidergic Neurons Enable Maternal Preparatory Nesting. Neuron in press.

Turek VF, and Ryabinin AE (2005). Ethanol versus lipopolysaccharide-induced hypothermia: involvement of urocortin. Neuroscience 133, 1021–1028. [PubMed: 15964490]

Vaughan J, Donaldson C, Bittencourt J, Perrin MH, Lewis K, Sutton S, Chan R, Turnbull AV, Lovejoy D, Rivier C, et al. (1995). Urocortin, a mammalian neuropeptide related to fish urotensin I and to corticotropin-releasing factor. Nature 378, 287–292. [PubMed: 7477349]

Warwick R (1954). The ocular parasympathetic nerve supply and its mesencephalic sources. J Anat 88, 71–93. [PubMed: 13129172]

Weitemier AZ, and Ryabinin AE (2005). Lesions of the Edinger-Westphal nucleus alter food and water consumption. Behav Neurosci 119, 1235–1243. [PubMed: 16300431]

Weitemier AZ, Tsivkovskaia NO, and Ryabinin AE (2005). Urocortin 1 distribution in mouse brain is strain-dependent. Neuroscience 132, 729–740. [PubMed: 15837134]

Westphal CFO (1887). Ueber einen Fall von chronischer progressiver Lahmung der Augenmuskeln (Ophthalmoplegia externa) nebst Beschreibung von Ganglienzellengruppen im Bereiche des Oculomotoriuskerns. Arch Psychiat und Nervenkrankheiten 18, 846–871.

Wong ML, al-Shekhlee A, Bongiorno PB, Esposito A, Khatri P, Sternberg EM, Gold PW, and Licinio J (1996). Localization of urocortin messenger RNA in rat brain and pituitary. Mol Psychiatry 1, 307–312. [PubMed: 9118356]

Xu L, Bloem B, Gaszner B, Roubos EW, and Kozicz T (2009). Sex-specific effects of fasting on urocortin 1, cocaine- and amphetamine-regulated transcript peptide and nesfatin-1 expression in the rat Edinger-Westphal nucleus. Neuroscience 162, 1141–1149. [PubMed: 19426783]

Xu L, Furedi N, Lutter C, Geenen B, Petervari E, Balasko M, Denes A, Kovacs KJ, Gaszner B, and Kozicz T (2022). Leptin coordinates efferent sympathetic outflow to the white adipose tissue through the midbrain centrally-projecting Edinger-Westphal nucleus in male rats. Neuropharmacology 205, 108898. [PubMed: 34861283]

Xu L, Scheenen WJ, Leshan RL, Patterson CM, Elias CF, Bouwhuis S, Roubos EW, Myers MG Jr., and Kozicz T (2011). Leptin signaling modulates the activity of urocortin 1 neurons in the mouse nonpreganglionic Edinger-Westphal nucleus. Endocrinology 152, 979–988. [PubMed: 21209012]

Zhang Z, Zhong P, Hu F, Barger Z, Ren Y, Ding X, Li S, Weber F, Chung S, Palmiter RD, et al. (2019). An Excitatory Circuit in the Perioculomotor Midbrain for Non-REM Sleep Control. Cell 177, 1293–1307 e1216. [PubMed: 31031008]

Zuniga A, and Ryabinin AE (2020). Involvement of Centrally Projecting Edinger-Westphal Nucleus Neuropeptides in Actions of Addictive Drugs. Brain Sci 10.

Zuniga A, Ryabinin AE, and Cunningham CL (2020). Effects of pharmacological inhibition of the centrally-projecting Edinger-Westphal nucleus on ethanol-induced conditioned place preference and body temperature. Alcohol 87, 121–131. [PubMed: 31926294]

Zuniga A, Smith ML, Caruso M, and Ryabinin AE (2021). Vesicular glutamate transporter 2-containing neurons of the centrally-projecting Edinger-Westphal nucleus regulate alcohol drinking and body temperature. Neuropharmacology 200, 108795. [PubMed: 34555367]

Highlights:

- The centrally-projecting Edinger-Westphal nucleus expresses oxytocin receptors.
- We confirm that urocortin neurons of EWcp are not glutamatergic.
- Exogenous oxytocin administration induces FOS in EWcp neurons.
- Oxytocin doses inducing FOS in EWcp lead to hypothermia.

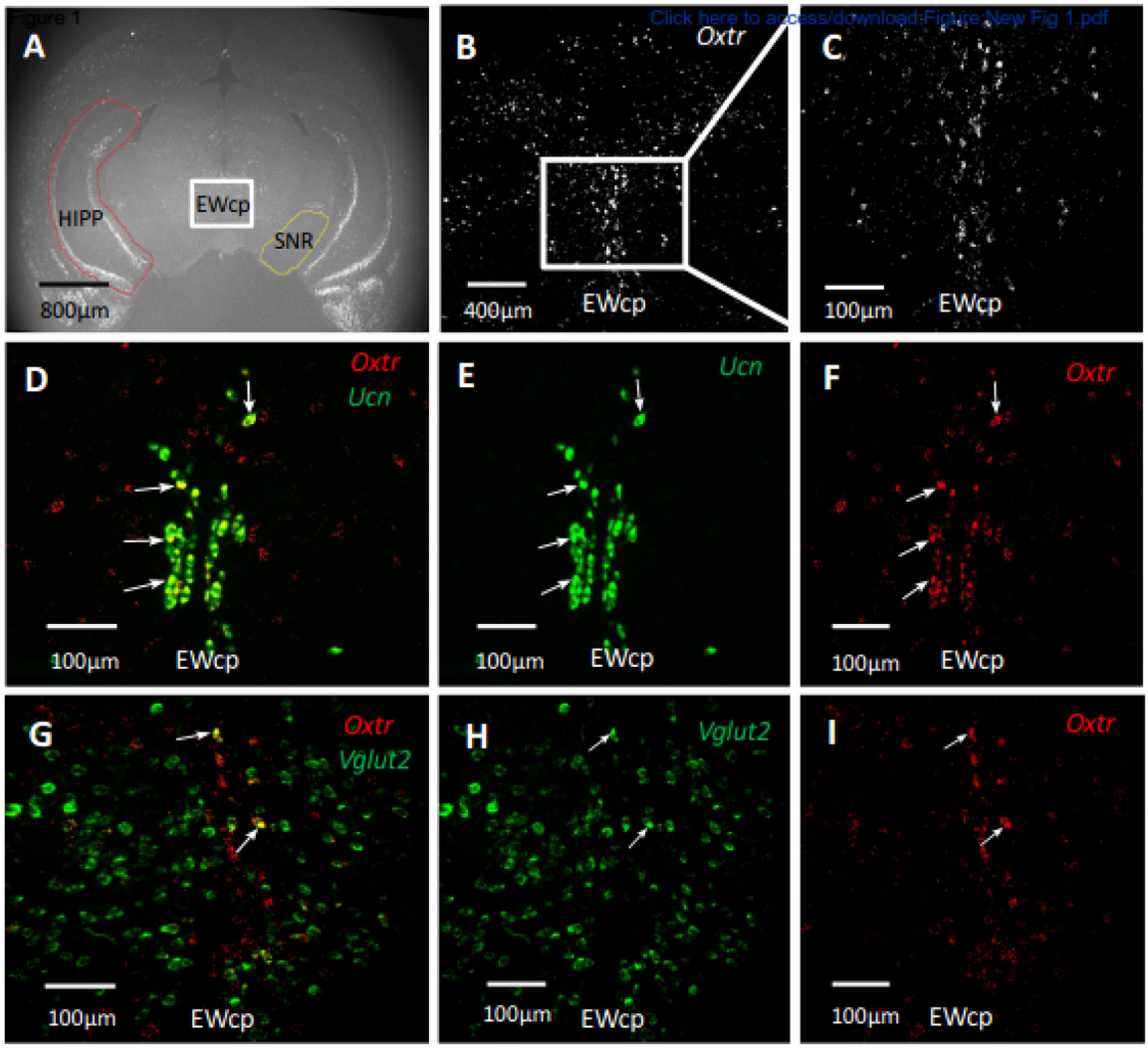

Figure 1. Oxytocin receptors in midbrain.

A. Oxytocin receptor (*Oxtr*) RNAscope in situ hybridization (ISH) in mouse brain at approximate Bregma position −3 mm at 2.5x objective magnification. The central rectangle outlines the EWcp. The hippocampus (HIPP) is outlined by a red line and substantia nigra (SNR) is outlined by a yellow line. **B**. A 5x objective magnification image of a subsection of *Oxtr* RNAscope ISH in mouse brain at Bregma position − 3 mm focusing on the EWcp area. **C**. A 20x objective magnification image of a subsection of *Oxtr* RNAscope ISH in mouse EWcp area. **D**. Double-labeling for *Oxtr* and urocortin 1 (*Ucn*) RNAscope ISH in the mouse EWcp area. Arrows point to complete colocalization of *Ucn* mRNA and *Oxtr* mRNA. **E**. Single channel of Double-labeling for *Oxtr* and *Ucn* RNAscope ISH in the mouse EWcp. Arrows point to complete colocalization of the two markers. **F**. Single channel image of *Ucn* RNAscope ISH in the mouse EWcp. **G**. Single channel image of *Vglut2* RNAscope ISH in the mouse EWcp. **H**. Double-labeling for *Oxtr* mRNA and vesicular glutamate transporter 2 (*Vglut2*) RNAscope ISH in the mouse EWcp. Arrows point to examples of occasional colocalization of *Vglut2* mRNA and *Oxtr* mRNA. **H**. Double-labeling for *Oxtr* and Vesicular glutamate transporter 2 (*Vglut2*) RNAscope ISH in the mouse EWcp area. Arrows point to

occasional examples of colocalization of *Oxtr* mRNA and *Vglut2* mRNA. **I**. Single channel image of *Vglut2* RNAscope ISH in the mouse EWcp. **J**. Single channel image of *Oxtr* RNAscope ISH in the mouse EWcp. III identifies the location of the oculumotor nucleus.

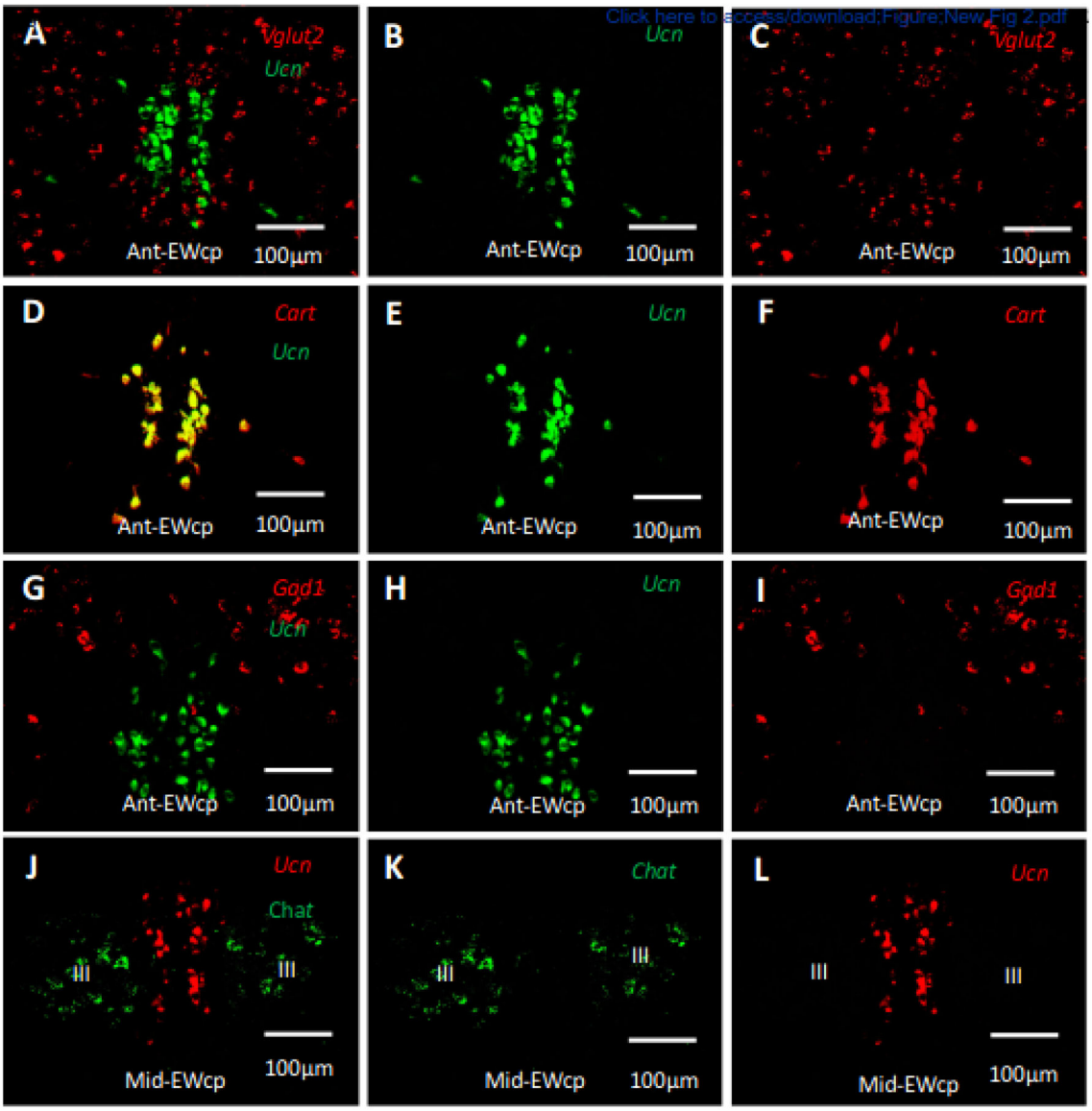

Figure 2. Examples of double labeling analysis by RNAscope ISH.

A, Merged image of *Vglut2* and *Ucn* signals in the anterior EWcp. No colocalization was observed. **B**, Single channel image of *Ucn* signal. **C**, Single channel image of *Vglut2* signal. **D**, Merged image of *Cart* and *Ucn* signals in the anterior EWcp. Note complete colocalization. **E**, Single channel image of *Ucn* signal. **F**, Single channel image of *Cart* signal. **G**, Merged image of *Gad1* and *Ucn* signals in the anterior EWcp. No colocalization was observed. **H**, Single channel image of *Ucn* signal. **I**, Single channel image of *Gad1* signal. **J**, Merged image of *Ucn* and *Chat* signals in the middle EWcp. No colocalization was observed. **K**, Single channel image of *Chat* signal. **L**, Single channel image of *Ucn* signal. III identifies the location of the oculumotor nucleus.

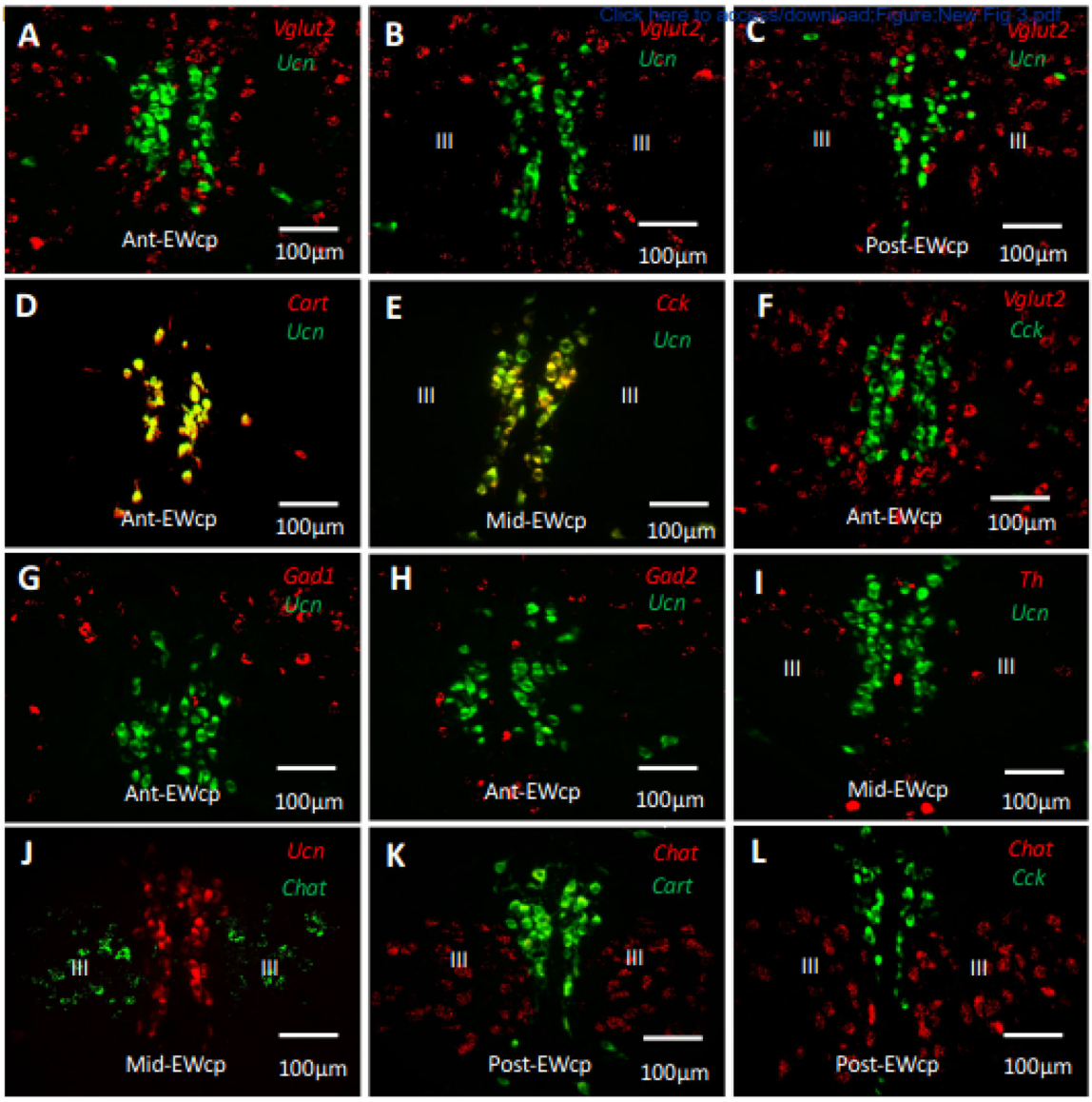

Figure 3. Characterization of neuronal subpopulations in the EWcp and its vicinity.

Double-labeling studies performed by RNAscope ISH. **A-C**. *Vglut2 and Ucn* in EWcp at three different Bregma levels: Anterior EWcp, middle EWcp and posterior EWcp. **D**. *Cart* and *Ucn* in the anterior EWcp. **E**. *Cck* and *Ucn* in the middle EWcp. **F**. *Vglut2* and *Cck* in the anterior EWcp. **G**. *Gad1* and *Ucn* in the anterior EWcp. **H**. *Gad2* and *Ucn* in the anterior EWcp. **I**. *Th* and *Ucn* in the middle EWcp. **J**. *Ucn* and *Chat* in the middle EWcp. **K**. *Chat* and *Cart* in the posterior EWcp. **L**. *Chat* and *Cck* in the posterior EWcp. III identifies the location oßf the oculumotor nucleus.

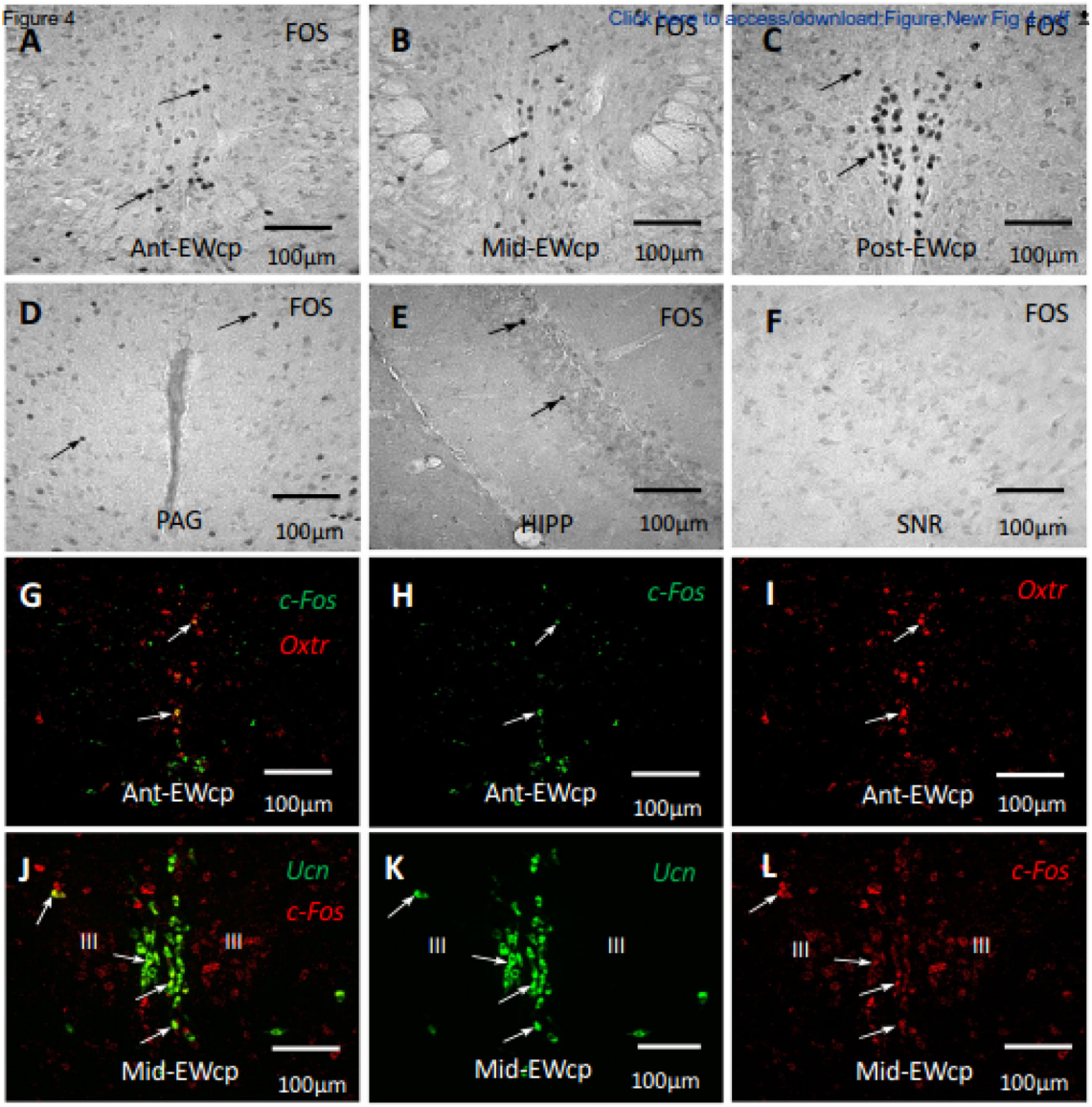

Figure 4. FOS response to exogenous OXT administration.

A-F. FOS immunohistochemistry following administration of 7.7 mg/kg OXT (IP) in EWcp (A-C), periaqueductal gray (D), hippocampus (E), substantia nigra (F). Black arrows indicate examples of FOS-positive cells. **G-I**. RNAscope ISH for *c-Fos* and *Oxtr* mRNA. **J-L**. RNAscope ISH for *c-Fos* and *Ucn* mRNA. White arrows indicate examples of colocalization. III identifies the location of the oculumotor nucleus.

Figure 5

Click here to access/download Figure New Fig 5.pdf

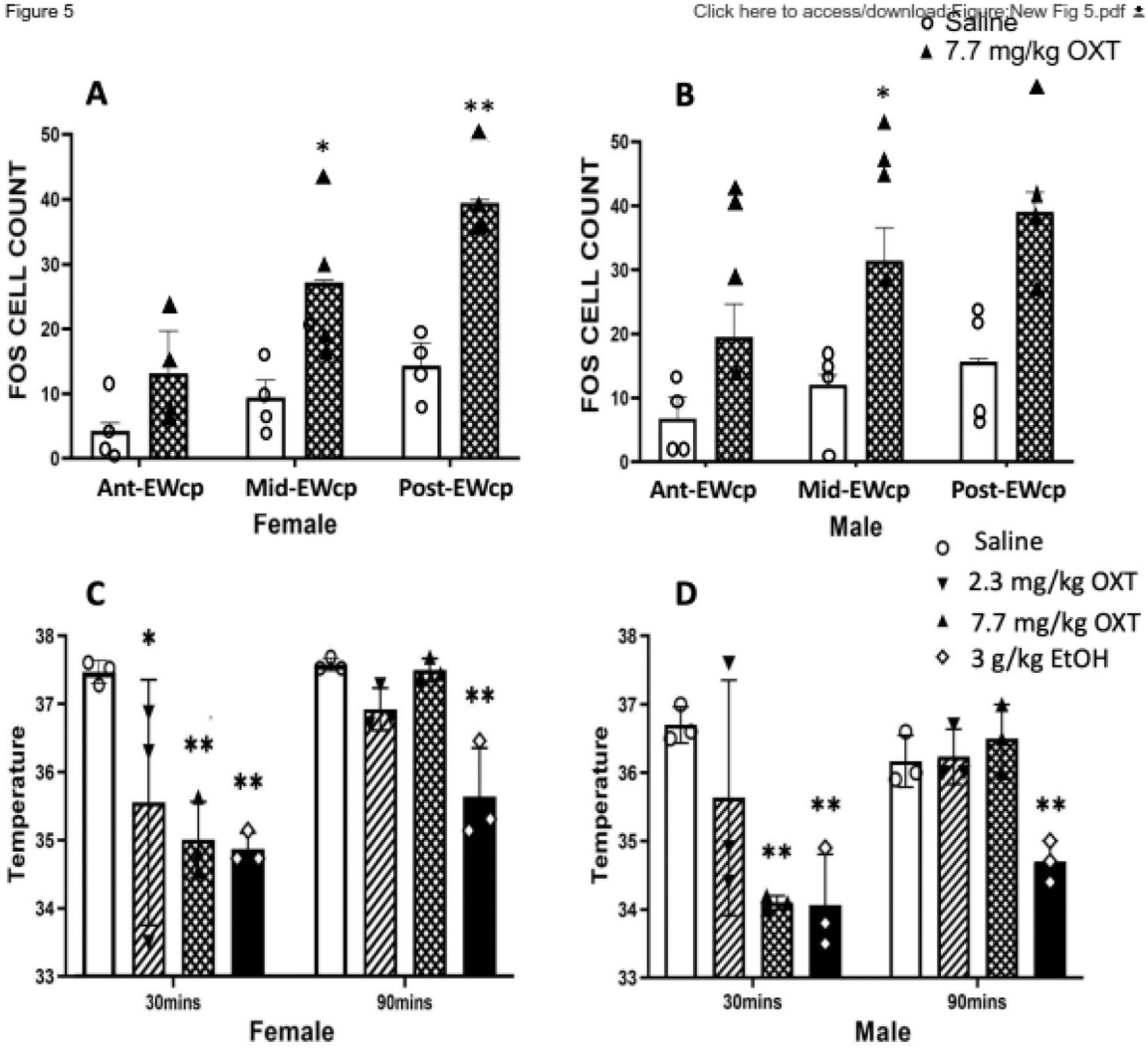

Figure 5. FOS induction and hypothermia after exogenous OXT administration.

A,B. Quantitative analysis of FOS immunoreactivity in EWcp following administration of 7.7 mg/kg OXT or saline in female (A) and male (B) mice across three Bregma levels. Post-hoc analyses: *p<0.05, **p<0.01 compared to corresponding saline group. **C,D**. Body temperature at 30 and 90 minutes after the injection of Saline, 2.3 mg/kg OXT, 7.7 mg/kg OXT or 3 g/kg of ethanol in female (C) or male (D) mice. Post-hoc analyses: *p<0.05, **p<0.01 compared to corresponding saline group.

Table 1.

Probes used in the study.

Probe name	Catalogue number
RNAscope® Probe- Mm-Ucn	466261
RNAscope Probe - Mm-Fos-C2	316921
RNAscope® Probe - Mm-Oxtr-C2	412171
RNAscope Probe - Mm-Slc17a6-C2 (Vglut2)	319171
RNAscope Probe - Mm-Chat-C2	408731
RNAscope Probe - Mm-Th-C3	317621
RNAscope Probe - Mm-Cck-C3	402271
RNAscope Probe - Mm-Cartpt-C3	432001
RNAscope Probe - Mm-Gad2-C3	439371
RNAscope Probe - Mm-Gad1-C3	400951
RNAscope Probe - Mm-Cck-C1	402271

Table 2.

Number of FOS-positive cells following injection of oxytocin or ethanol and body temperature measurements.

	Sex	Saline	2.3 mg/kg Oxt	p=	7.7 mg/kg Oxt	p=	3 g/kg EtOH	p=	2-way ANOVA
Ant-EWcp	F	2.22±0.29	5.89±2.08	.053	8.89±1.44	**.034**	27.22±2.80	**<.001**	Bregma level: $F_{2,32}$=17.21, p<0.001, $\eta 2$=0.58 Bregma level × treatment: $F_{6,32}$=3.81, p=0.006, $\eta 2$=0.42
	M	2.00±0.58	9.67±3.15		7.89±1.16		15.89±3.75		
Mid-EWcp	F	1.89±0.40	13.33±6.36	**.031**	9.11±3.58	.057	31.89±6.15	**<.001**	
	M	1.56±0.48	10.89±4.39		12.44±3.62		21.56±6.78		
Post-EWcp	F	2.22±0.29	5.89±2.08	**.006**	14.67±2.87	**.018**	37.89±3.50	**<.001**	
	M	1.00±0.38	16.78±5.76		14.00±5.36		37.00±10.22		

p values indicate LSD differences from the Saline group. Since there were no significant effects of sex and no significant sex by treatment interactions, post-hoc PLSD analyses were performed with data collapsed across sex. $\eta 2$ indicates effect size.